

Invited commentary

## Mechanical strength testing of compacted powders

Peter Stanley \*

*The Manchester School of Engineering, Simon Building, University of Manchester, Oxford Road, Manchester M13 9PL, UK*

Received 21 February 2001; accepted 17 March 2001

---

### Abstract

Alternative test specimens for the determination of the fracture stress of brittle materials (eg. compacted powders) are described and discussed, and a statistical approach to the processing of strength test data is outlined. © 2001 Elsevier Science B.V. All rights reserved.

**Keywords:** Fracture stress; Mechanical properties; Test specimens; Strength testing

---

### 1. Introduction

An important characteristic of powder compacts is that they are brittle, i.e. in contrast with a ductile material (e.g. mild steel) fracture is not preceded by significant permanent deformation. For this reason, the simple tensile specimen widely used in the strength testing of metals is not ideal for these materials and is rarely, if ever, used. (The principal difficulty is the avoidance of premature failure associated with stress increases due to misalignment of the specimen in the loading attachments or to contact effects of the attachments themselves.) Consequently, alternative specimens must be sought.

An essential feature of a satisfactory test specimen is that the geometry and loading must be such that a calculable stress state prevails at the

section where fracture occurs so that the fracture stress can be readily calculated from the fracture load. It is also desirable that the specimen is simple and that the minimum is required by way of shackles, grips, attachments etc. for loading. (It is assumed that a satisfactory standard load-applying machine is available.) Several suitable specimens are described and discussed below.

### 2. The beam

The beam is a geometrically simple specimen, easily made and readily loaded. Load alignment problems are eliminated by the use of a simple fixture or jig in which the beam is supported on and loaded through smooth hard cylindrical rollers.

The beam specimen can have any cross-sectional shape, but for convenience, sections with at

---

\* Tel.: +44-161-275-4303; fax: +44-161-275-4346.

least one plane of symmetry are preferred. The rectangular cross-section is generally easy to make as a compact though many brittle products are available with hollow or solid cylindrical cross-sections (e.g. glass tubing, quartz and silica ware, fire-clay ware) or isosceles-triangular cross-sections. Typically, the length of the beam should be at least ten times the cross-sectional dimension, though stubbier 'beams' are tested (David and Augsburger, 1974). With this proviso, the absolute size of the specimen can range from something like a match-stick to a railway sleeper, depending on the particle size of the powder, the strength of the compact and the sensitivity and load capacity of the test machine.

The relevant theory is developed in the standard textbooks (Case et al., 1993; Benham et al., 1996); it is summarised here for reference. A rectangular cross-section ( $b \times d$ , breadth  $\times$  depth) is assumed for convenience. The modifications necessary for singly symmetric or asymmetric cross-sections are readily introduced.

The longitudinal stress  $\sigma$  due to a bending moment  $M$  at a particular section of a beam (Fig. 1) is given by

$$\sigma = \frac{M}{I} y \quad (1)$$

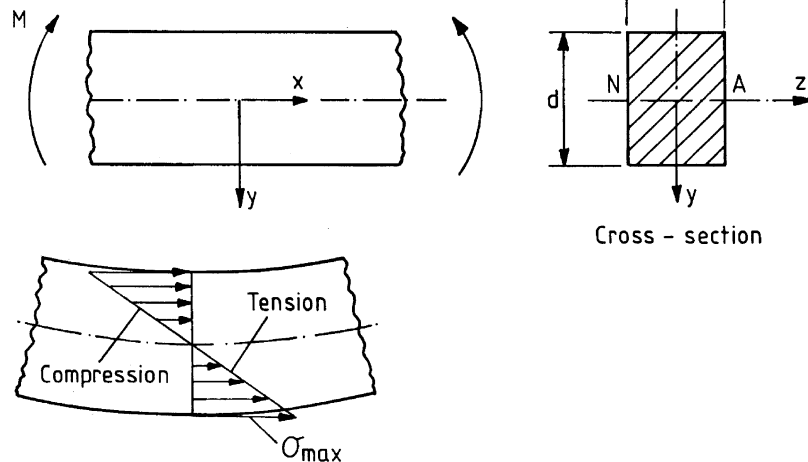


Fig. 1. Beam bending.

where  $y$  is the transverse co-ordinate measured in the plane of bending (Fig. 1) and  $I$  is the second moment of area of the cross-section about the neutral axis ( $NA$ ; see Fig. 1). From Eq. (1) it can be seen that  $\sigma$  varies linearly across the section from a maximum tensile stress on the lower face (in the case shown) through zero along the centre line to a numerically equal compressive stress on the upper face. (Linear elastic behaviour is assumed. Shear effects on the section may modify the overall stress distribution but will not affect the surface maxima. Stresses in the  $z$ -direction are taken as zero.)

It follows from Eq. (1) that

$$\sigma_{\max} = \frac{M d}{I 2} \quad (2)$$

In practice, one of two alternative loading models is used; 3-point loading (Fig. 2a) or 4-point loading (Fig. 2b). Fracture occurs when the applied load is such that the maximum stress  $\sigma_{\max}$  equals the tensile fracture stress of the material. The relationships necessary for obtaining the tensile fracture stress of the material from the total applied load at fracture are tabulated below (Table 1).

The possible effects of friction at the loading and support points may require consideration. If

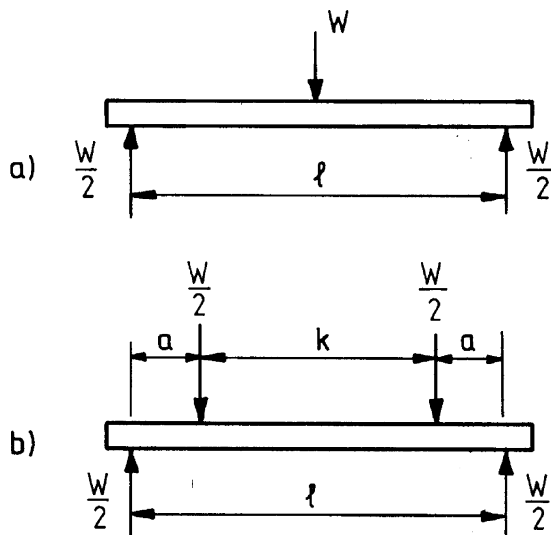


Fig. 2. Loading modes for bend tests. (a) 3-point, (b) 4-point.

suitable bearings are incorporated in the loading support rig, frictional effects can be practically eliminated. A detailed treatment of these effects is given in Stanley et al. (1976) and a 'tandem' testing arrangement in which such frictional effects are practically eliminated is described by Stanley and Inanc (1984).

### 3. The 'Brazilian' disc

The simple plane-faced disc specimen subjected to two diametrically opposed point loads (Fig. 3)

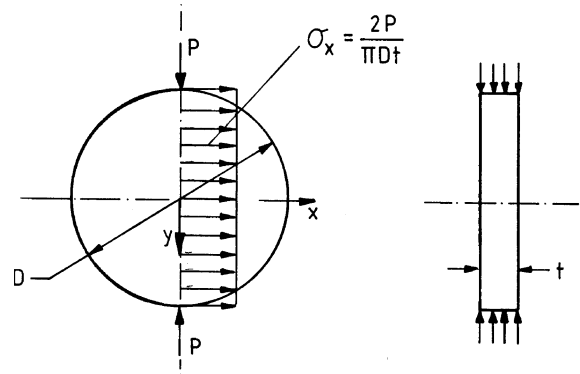


Fig. 3. The 'Brazilian' disc.

is widely used for the determination of the tensile fracture stress of brittle compacts (Fell and Newton, 1970). The test was devised originally by two Brazilian engineers (Carneiro and Barcellos, 1953) and is referred to as the 'indirect' tensile test—the adjective 'indirect' arising presumably to cover the apparent anomaly of deriving the tensile fracture stress from compressive loading. Again, there are no significant manufacturing or loading problems. The ratio of specimen thickness to diameter is usually within the 0.25–0.5 range. The size range is governed by the factors mentioned above for the beam specimen, with 10 mm or possibly somewhat less as a lower limit. For the test, the specimen is simply placed between the two parallel flat platens of a conventional test machine with no need for elaborate fixtures or grips.

Table 1  
Formulae for use with beam specimens

	Rectangular section		Solid circular section	
	3-point loading	4-point loading	3-point loading	4-point loading
$M_{\max}$	$\frac{Wl}{4}$	$\frac{Wa}{2}$	$\frac{Wl}{4}$	$\frac{Wa}{2}$
$I$	$\frac{bd^3}{12}$	$\frac{bd^3}{12}$	$\frac{\pi}{64} D^4$	$\frac{\pi}{64} D^4$
$\sigma_f$	$\frac{3l}{2bd^2} W_f$	$\frac{3a}{bd^2} W_f$	$\frac{8l}{\pi D^3} W_f$	$\frac{16a}{\pi D^3} W_f$

$W$ , total applied load;  $W_f$ ,  $W$  at fracture;  $a$ , see Fig. 2(b);  $l$ , distance between supports (Fig. 2; not length of beam);  $b$ , breadth of rectangular cross-section (Fig. 1);  $d$ , depth of rectangular cross-section (Fig. 1);  $D$ , diameter of solid circular cross-section;  $\sigma_f$ , tensile fracture stress of material.

A feature of this specimen is that there is a complete analytical solution (Den Hartog, 1952) for the stress state induced by the loads. (Departures from the analytical stress solution in the immediate vicinity of the two points of load application are usually of no consequence.) It transpires that the loaded diameter of the specimen experiences a transverse tensile stress, which is uniform along the length of the diameter.

In terms of the load  $P$ , the diameter  $D$ , the thickness  $t$  and co-ordinates  $x$  and  $y$  (Fig. 3), the stresses  $\sigma_x$  and  $\sigma_y$  along the vertical and horizontal diameters of the specimen are:

Vertical diameter:

$$\sigma_x = \frac{2P}{\pi Dt} \quad (3.1)$$

$$\sigma_y = \frac{2P}{\pi Dt} \left[ 1 - \frac{4D^2}{D^2 - 4y^2} \right] \quad (3.2)$$

Horizontal diameter:

$$\sigma_x = \frac{2P}{\pi Dt} \left[ 1 - \frac{16x^2 D^2}{(D^2 + 4x^2)^2} \right] \quad (3.3)$$

$$\sigma_y = \frac{2P}{\pi Dt} \left[ 1 - \frac{4D^4}{(D^2 + 4x^2)^2} \right] \quad (3.4)$$

Stresses normal to the plane of the specimen are assumed to be zero unless the specimen thickness is comparable with or greater than the diameter. Although the compressive stresses (indicated by a minus sign) are generally considerably higher than the tensile stresses, the ratio of tensile to compressive strength of these materials is such that fracture usually occurs along the vertical diameter as a result of the uniform tensile stress  $2P/\pi Dt$  acting normal to that diameter. Consequently, for such fractures, the tensile fracture stress  $\sigma_f$  is readily obtained from the fracture load  $P_f$  as  $2P_f/\pi Dt$ .

Anomalous results can be obtained from this test when the material is relatively soft or when the shear strength of the material is relatively low. Various adaptations have been studied, including the effect of distributed loading (Hondros, 1959) and the use of shaped platens (or ' anvils') (Awaji and Sato, 1979). It is important to note a signifi-

cant distinction between the tensile fracture stress obtained from the beam test and that obtained from the Brazilian disc test; the former pertains to a strictly uniaxial stress state whilst the latter is associated with a transverse compressive stress considerably greater than the tensile stress. As a generalisation, it can be said (see later) that the tensile fracture stress obtained from the beam test (i.e. the uniaxial stress condition) will be greater than that derived from the disc test (a biaxial stress condition).

#### 4. Disc with traverse loading

The plane disc specimen can be loaded in bending (Stanley and Sivill, 1978) to provide a useful counterpart to the 3-point and 4-point beam specimens. In this loading mode, the disc is uniformly supported on a concentric circular ring and loaded by either a point load at the centre (Fig. 4a) or via a second concentric ring (Fig. 4b). A thickness to diameter ratio of the order 1 to 10 is preferable; the design of a suitable specimen loading jig is straightforward (Fig. 5).

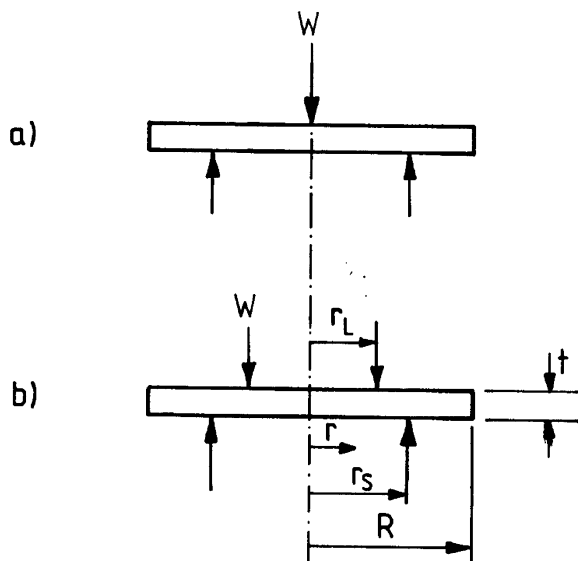


Fig. 4. Disc bending. (a) Point-loaded, ring-supported, (b) ring-loaded, ring-supported.

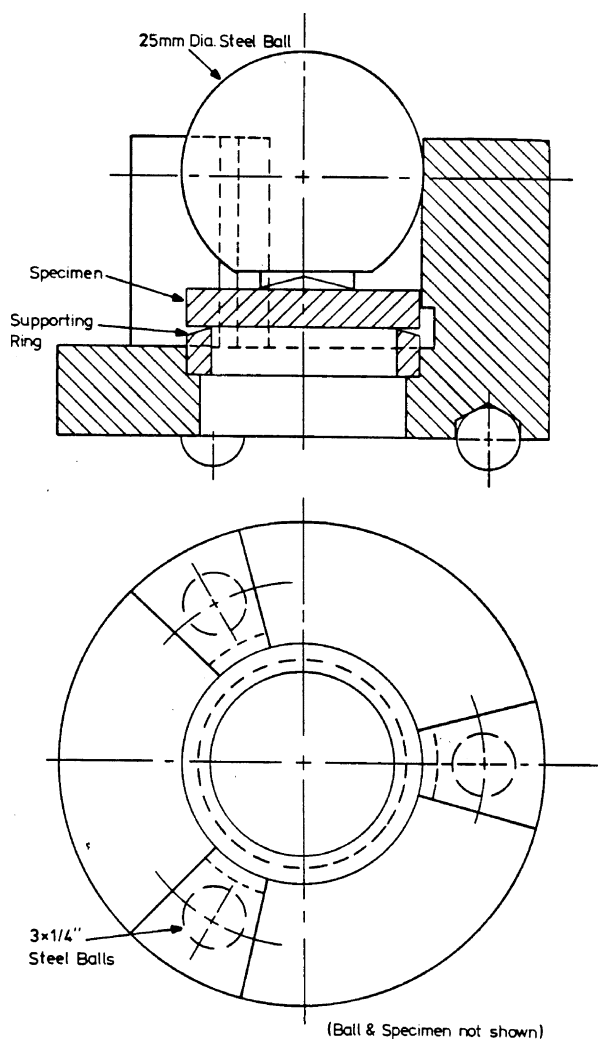


Fig. 5. Disc loading jig.

Analytical stress solutions are available (Den Hartog, 1952) for both forms of loading, but that for the point-loaded disc can present difficulties and the ring-loaded alternative is to be preferred. Within the central portion of the ring-loaded, ring-supported disc specimen (i.e. for  $r < r_L$ —see Fig. 4b) there is a uniform equi-biaxial stress state which varies linearly from tension on the lower surface through zero on the mid-surface to compression on the upper surface. The lower surface tensile stress in the specimen is related to the applied load  $W$  and the specimen dimensions (see Fig. 4) by the expression

$$\sigma = \left[ \frac{3W}{2\pi t^2} (1 - \nu) \frac{r_S^2 - r_L^2}{2R^2} + (1 - \nu) \ln \frac{r_S}{r_L} \right] \quad (4)$$

where  $\nu$  is the Poisson's ratio (Case et al., 1993) of the material. (Other symbols are defined in Fig. 4b.) Using this equation, the tensile fracture stress  $\sigma_f$  is readily obtained from the fracture load  $W_f$  provided Poisson's ratio is known or a value can be assumed for it. (Commonly assumed values are in the range 0.3–0.5.)

Again, the value of the tensile fracture stress obtained from this test is not to be seen as strictly equivalent to that obtained from beam tests or the Brazilian disc test (see later); the value relates to the equi-biaxial stress condition and is referred to as the equi-biaxial tensile fracture stress.

The above  $\sigma - W$  equation is not over-sensitive to small changes in Poisson's ratio, but because of the occurrence of  $\nu$  in the equation the ring-loaded ring-supported test is perhaps more useful in a comparative study where changes in the fracture stress are required rather than absolute values. The point-loaded ring-supported disc can also be used in such studies. A related test mode, in which the disc specimen is symmetrically supported on three balls and loaded centrally through a fourth (the 'four ball' test), may also warrant consideration in such work (Stanley, 1992).

## 5. Shear strength test

The conventional shear specimen takes the form of a tube or solid cylindrical bar subjected to a torque loading. This form of testing is not ideal for a brittle material and an alternative has been developed (Rabie, 1981) in which a beam specimen is used. The arrangement is shown schematically in Fig. 6. In practice, a simple jig may be used. The specimen consists of a simple symmetrically notched beam of rectangular cross-section. The loading is such that the central section of the specimen experiences zero bending moment but a shear force of  $Wa/(l - a)$ . As a result of the two  $90^\circ$  notches (with the notch depth equal to one quarter of the full section depth,  $d$ ) this shear force is distributed across section  $AA$  (see Fig. 6) as a uniform shear stress of magnitude  $Wa/[bd(l - a)]$ , where  $b$  is the breadth of the specimen

and  $d'$  is the section depth between the notch roots. The shear fracture stress  $\tau_f$  is thus readily derived from the fracture load  $W_f$ .

Experience has shown that, depending upon the loading details, some specimen development may be necessary to ensure that failure occurs in shear rather than in bending. Nevertheless, this form of testing has considerable advantages over torsion testing and is becoming accepted as a valuable alternative to it.

## 6. The 'fracture envelope' concept

The 'fracture envelope' representation of the strength characteristics of a particular material affords a rational basis for the comparison and appraisal of the distinctive strength values obtained from the four tests described above.

An element of material subjected to two independent orthogonal 'in-plane' principal stresses,  $\sigma_1$  and  $\sigma_2$  (Fig. 7a), is considered. A combination of  $\sigma_1$  and  $\sigma_2$  which causes fracture can be represented as a point in a co-ordinate system with Cartesian axes  $\sigma_1$  and  $\sigma_2$ .

The full range of such combinations represented in this way defines the 'fracture envelope' of the material. Possible forms of 'fracture envelope' are shown schematically in Fig. 7(b) as the polygon  $a b a c d c a$  or as the closed curve  $a b' a c d' c a$ . The basic feature of the 'fracture envelope' is that stress states represented by points within the envelope can be sustained by the

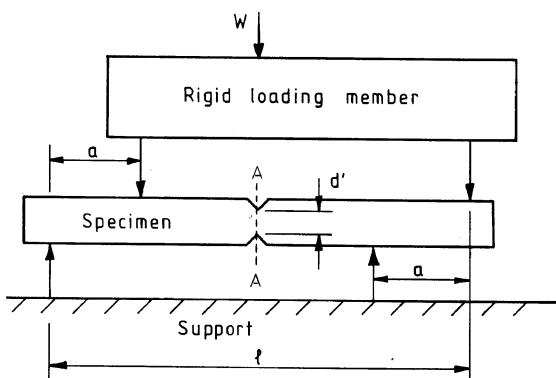


Fig. 6. Shear strength test.

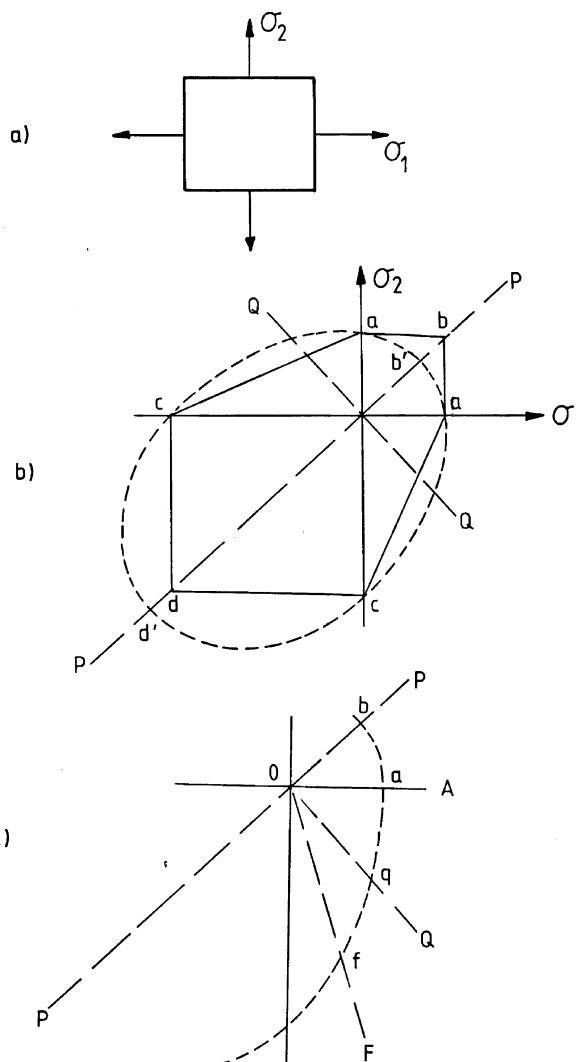


Fig. 7. The 'fracture envelope'. (a) biaxial stress state, (b) possible forms, (c) construction.

material without fracture, stress states represented by points on the envelope will cause fracture and stress represented by points outside the envelope cannot be sustained by this material. An important detail of the fracture envelope for an isotropic brittle solid is that it is symmetrical about the line  $PP$  (Fig. 7b); it is not, in general, symmetrical about the line  $QQ$ , the strength in compression being greater than that in tension.

Some generalisations have been proposed (Pridde, 1969; Dukes, 1971; Stanley and Sivill, 1978)

but the determination of the detailed shape of the fracture envelope for a particular material requires an extensive experimental study designed so that  $\sigma_1$  and  $\sigma_2$  can be controlled independently over a wide range of values. Fracture stress values derived for a particular material from the tests described above give a number of key points on the fracture envelope (see Fig. 7(c) in which symmetry about  $PP$  is assumed):

1. Beam bending gives the uniaxial tensile fracture stress and therefore defines point  $a$  on the principal stress axis  $OA$ .
2. The Brazilian disc test gives a point in the lower part of the tension–compression quadrant. The ‘ $x$ ’ co-ordinate of the point is obtained directly from the test. There is some uncertainty in the ‘ $y$ ’ co-ordinate, but it is at least three times the ‘ $x$ ’ co-ordinate. The point can be positioned, somewhat arbitrarily, along the line  $OF$  which has a slope of  $-3$ .
3. The ring-loaded, ring-supported test provides the equi-biaxial tensile fracture stress and therefore defines point  $b$  on the symmetry line  $PP$ .
4. The pure shear condition is equivalent to equal and opposite principal stresses (each equal in magnitude to the shear stress). The shear test therefore defines the point  $q$  along the line  $OQ$  perpendicular to  $PP$ . Clearly, a complete definition of the envelope would require work in the compression—compression quadrant.

The fracture envelope provides a valuable conceptual aid in fracture studies. Developments for anisotropic materials and three-dimensional stress states are important.

## 7. Statistical treatment

It might be inferred from the foregoing that, within the limits of acceptable experimental error, an individual fracture stress value obtained from one of the tests described above is definitive and unique. This is not so.

Within a brittle material, there is a multitude of microscopic structural and material defects in the form of interstitial cavities, fractured particles, inter-particular boundaries, etc. These defects act

as minute stress concentrations in the material and as the applied load is increased, fracture will initiate and propagate from one of them. Since the defects are randomly distributed throughout the material and are of random severity, there is an inevitable inherent variability in the strength of nominally identical brittle specimens over and above that which may be present because of variations in composition or details of manufacture. This variability requires that strength test results for brittle materials are treated statistically; the Weibull probability distribution (Weibull, 1951) is usually used for this purpose.

The form of the distribution used (Stanley and Newton, 1977) is

$$P_f = 1 - \exp \left[ - \left( \frac{1}{m} \right)^m \left( \frac{\sigma}{\bar{\sigma}_f} \right)^m \right] \quad (5)$$

where  $P_f$  is the cumulative probability of failure associated with the stress  $\sigma$ ,  $\bar{\sigma}_f$  is the mean fracture stress and  $m$  is the Weibull modulus of the material. The term  $((1/m)!)$  is the ‘ $\gamma$ ’ function of  $((1/m) + 1)$  and is readily obtained from standard tables (Dwight, 1961).

The Weibull modulus  $m$  is a reciprocal measure of the strength variability of a brittle material and is to be seen as an important material characteristic, complementary to the fracture strength.

Plots of failure probability as a function of normalised stress, derived from Eq. (5) for various values of  $m$ , are shown in Fig. 8. It can be seen that the smaller  $m$ , the ‘flatter’ the curve and the greater the variability in strength. In view of this inherent variability, it is essential that batches of nominally identical specimens be tested rather than individual specimens, so that good average strength values and measures of the associated ‘spread’ or variability (i.e. the modulus  $m$ ) can be obtained.

The processing of the results from a batch of nominally identical test specimens (28 discs of  $\alpha$ -lactose monohydrate B.P.) is described in detail by Stanley and Newton (1977). Fig. 9 shows test results for a typical batch for which the derived  $m$  value was 9.8. The mean fracture stress  $\bar{\sigma}_f$  is readily obtained directly from the test data. Several alternative ways of determining  $m$  from test results are available (Kennerley et al., 1982); a

convenient approximation gives  $m$  in terms of the mean fracture stress ( $\bar{\sigma}_f$ ) and the Standard deviation ( $s$ ) of the test data:

$$m = 1.2 \frac{\bar{\sigma}_f}{s} \quad (6)$$

A further consequence of the brittle nature of powder compacts is that the mean fracture stress of a batch of specimens is size-dependent.

The larger the specimen the more likely it is that it will contain a flaw of a given severity and consequently the smaller will be the mean fracture stress of a batch of such specimens. The theoretical relationship between the mean fracture stresses and volumes of two batches A and B of geometrically similar specimens of different size is

$$\frac{\bar{\sigma}_{fA}}{\bar{\sigma}_{fB}} = \left( \frac{V_B}{V_A} \right)^{1/m} \quad (7)$$

Some work (Stanley and Newton, 1977) indicates that this relationship is not entirely adequate in accounting for the size-dependence of tablet strength.

Further developments of the Weibull-based statistical treatment are described by Stanley et al.

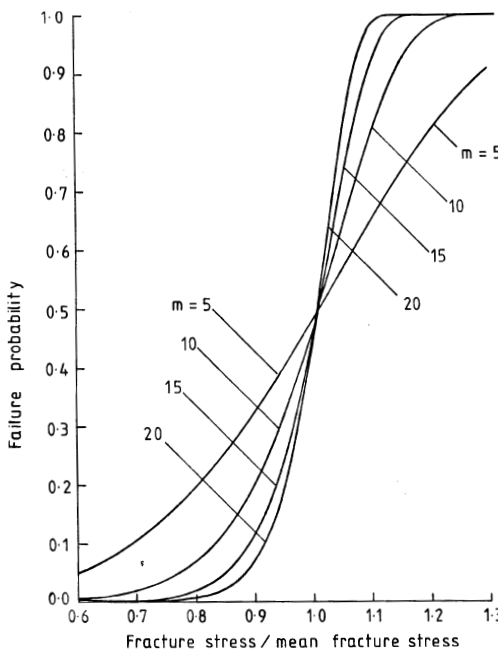


Fig. 8. Failure probability versus normalised stress.

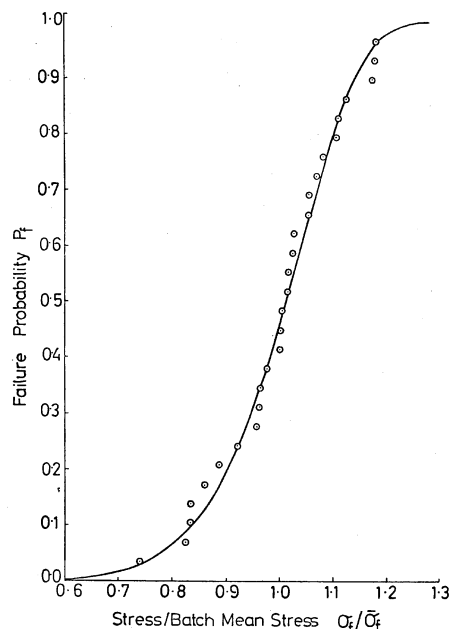


Fig. 9. Weibull plot for typical test batch.

(1976), Stanley and Newton (1977) and Kennerley et al. (1982). Stanley and Karroum (1992) describe work in which several strength test specimens for brittle materials are evaluated; graphite was used in this work as a representative material.

## 8. Properties related to stiffness

Other possibly relevant mechanical properties, relating to stiffness rather than strength, are Young's modulus ( $E$ ), Poisson's ratio ( $\nu$ ) and the shear modulus ( $G$ ).

Young's modulus is defined as the ratio of stress ( $\sigma$ ) to strain ( $\epsilon$ ) in a uniaxial stress system. In terms of the increase in length ( $\Delta l$ ) of a simple tensile specimen length  $l$ , cross-sectional area  $A$ , subjected to a tensile force  $F$

$$E = \frac{F/A}{\Delta l/l} \quad (8)$$

However, since simple tensile testing is impracticable for the materials under consideration, Young's modulus is best obtained from deflection measurements on a beam specimen.

A 4-point loaded beam (Fig. 2b) is considered. Expressions for the bending moment and the maximum stress within the central position of the beam have been given previously. An expression for the surface tensile strain in the central portion of the beam is available (Church, 1984), in terms of  $\delta$ , the deflection of the midpoint of the beam relative to the support points. From these expressions, the following relationship for Young's modulus is derived:

$$E = \frac{W}{\delta} \frac{6a}{bd^3} \left( \frac{k^2}{8} + \frac{ak}{2} + \frac{a^2}{3} \right) \quad (9)$$

( $a$  and  $k$  are defined in Fig. 2b.)

$E$  therefore is readily obtained from the gradient of the  $W$  (total load) versus  $\delta$  (central deflection) plot for the 4-point beam.

Poisson's ratio ( $\nu$ ) is defined as (minus) the ratio of the lateral strain to the longitudinal strain in a simple tensile specimen. It is not easy to determine Poisson's ratio directly. A method has been developed (Church, 1984) based on the measurement of the central deflection of a ring-loaded, ring-supported disc, but an indirect determination involving the measurement of the shear modulus ( $G$ , see below) is attractive. The relevant relationship (Case et al., 1993) is

$$\nu = \frac{E}{2G} - 1 \quad (10)$$

from which  $\nu$  is readily obtained in terms of  $E$  and  $G$ .

The shear modulus  $G$  is defined as the ratio of shear stress to shear strain and the simplest loading mode for test purposes is the torque loading of a cylindrical bar (Fig. 10). In such a test, it is readily shown (Case et al., 1993) that

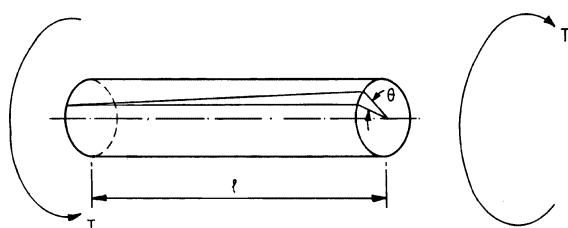


Fig. 10. Torque loading of cylindrical bar.

$$G = \frac{32l}{\pi d^4} \frac{T}{\theta} \quad (11)$$

where  $T$  is the applied torque,  $\theta$  the angle of twist,  $l$  the length of the bar and  $d$  the diameter.  $G$  is obtained directly from the gradient of a plot of  $T$  versus  $\theta$ .

## 9. Arbitrarily shaped compacts

It has been assumed in the foregoing that there is freedom of choice in the shape and size of the specimen. If it becomes necessary to test a compact of a specified non-simple shape (e.g. capsule-shaped, lozenge-shaped, convex-faced discs, grooved discs) a different approach must be adopted. Several possibilities are available. An approximate analysis has been used in a study of the fracture stress of capsule-shaped tablets (Stanley and Newton, 1980) and the material strength of double-convex aspirin tablets has been determined (Pitt et al., 1989a) using a non-dimensional stress factor obtained from fracture tests on gypsum compacts (Pitt et al., 1988; Stanley, 1991). More generally, however, whilst the determination of the fracture load of a non-standard brittle specimen under an agreed form of loading presents no problems, the derivation of the fracture stress of the material requires that the stresses induced in the compact by the applied load are known; a stress analysis is required and it is assumed that a simple analytical solution is not available.

Numerical or experimental methods can be used in these circumstances. The finite element method (Astley, 1992) is a powerful numerical technique in which the body is 'idealised' in the form of a 'mesh' of elements; several packages are commercially available for this purpose. An attractive experimental approach is by way of the three-dimensional photoelastic technique (Durelli and Riley, 1965) (i.e. the 'frozen-stress' technique) in which the stress distribution in a stress-birefringent model is deduced from the optical interference fringes in the loaded model. The model has to be geometrically similar to the compact; the model material is usually Araldite. The necessary experimental techniques are well established (Stanley, 1977).

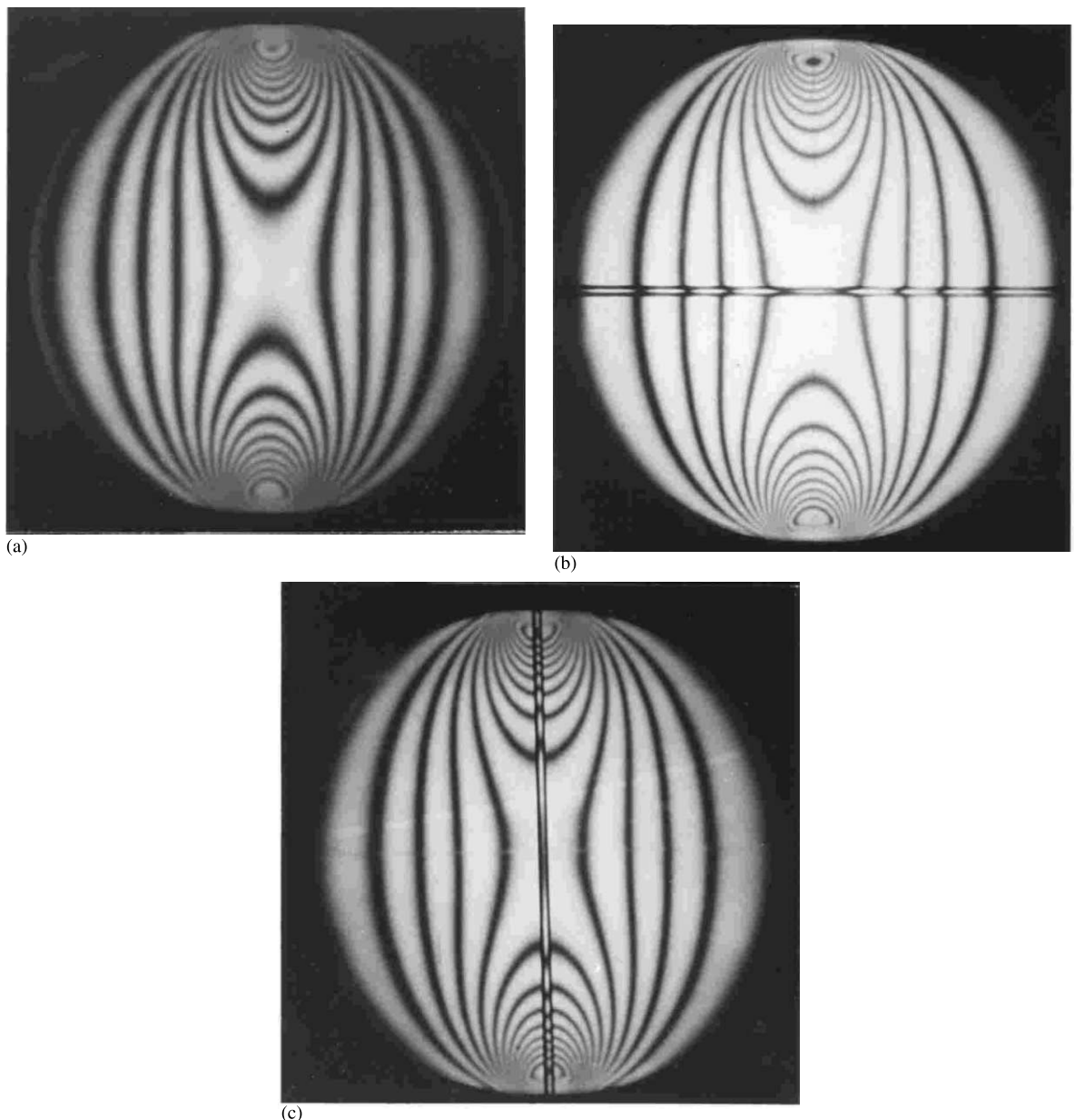


Fig. 11. Photoelastic fringes in plane and grooved discs. (a) plane-faced disc; (b) plane-faced disk with horizontal groove; (c) plane-faced disc with vertical groove.

Examples of such interference fringe patterns are shown in Figs. 11 and 12. Fig. 11 shows the photoelastic fringes in a disc subjected to diametrically opposed compressive loads, (a) with plane faces, (b) with a horizontal groove and (c) with a

vertical groove. Analysis of these patterns provides detailed stress data for the grooved tablet. Fig. 12 shows the photoelastic fringes in a series of rectangular plates subjected to opposed in-plane compressive loads. The variation of the maximum

tensile stress in this series of rectangular plate models as the width to height ratio is varied is shown in Fig. 13.

Further photoelastic work on the doubly-convex disk is described by Pitt et al. (1989b).

Having established the stress distribution in the compact, in deriving the fracture stress from the

fracture load, careful regard must be given to the effects of stress biaxiality, as outlined in Section 6.

## 10. Conclusion

A number of test specimens suitable for the determination of the mechanical strength of com-

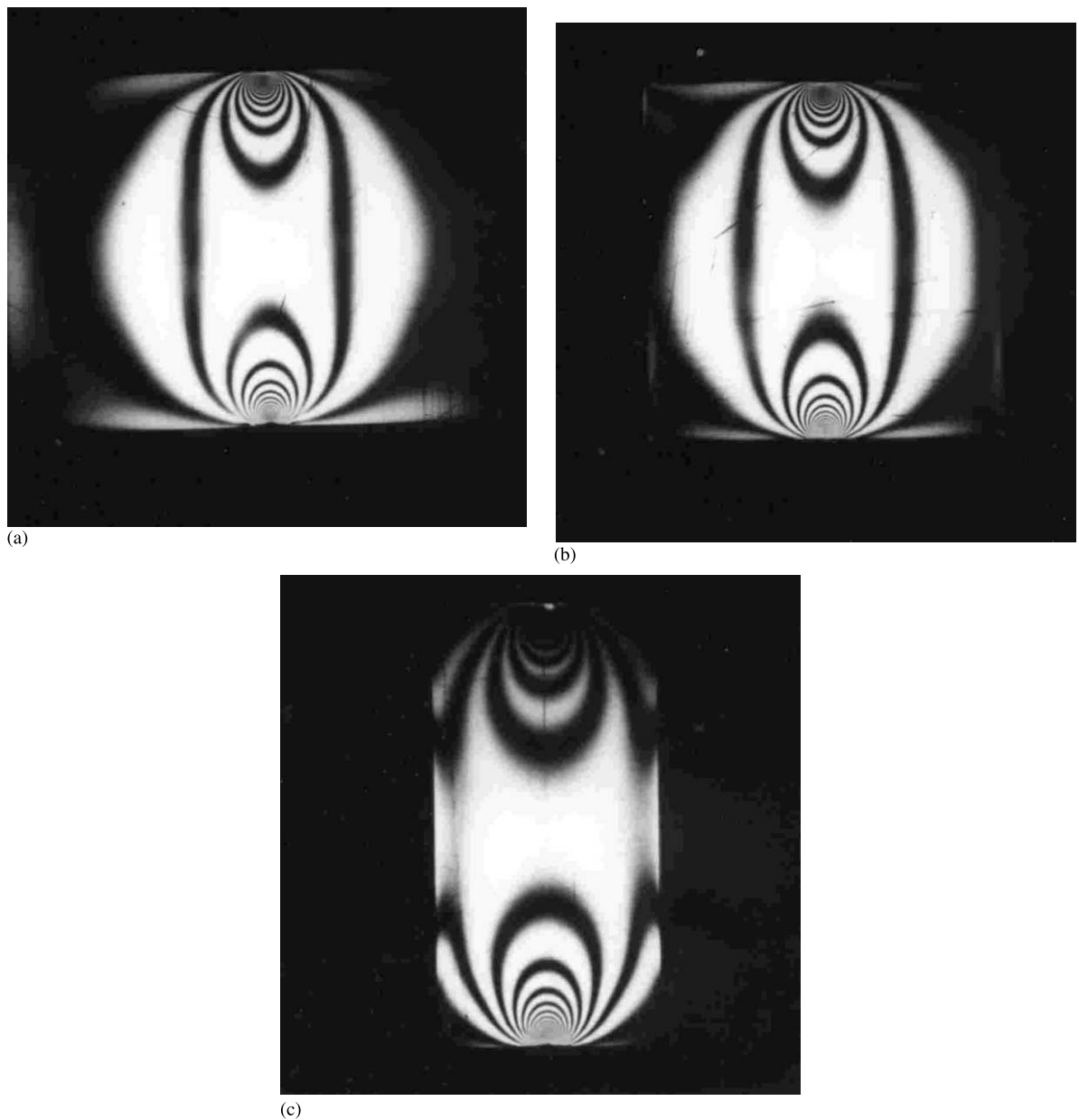


Fig. 12. Photoelastic fringes in rectangular plates.  $a$ , width;  $b$ , height. (a)  $a/b = 1.5$ , (b)  $a/b = 1.0$ , (c)  $a/b = 0.5$ .

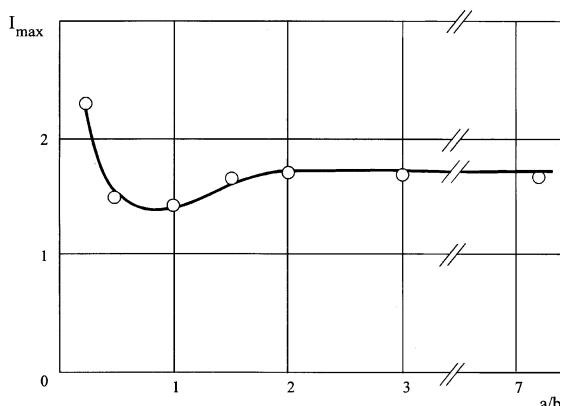


Fig. 13. Variation of maximum tensile stress with  $a/b$ .

pacted materials have been described and critically discussed. They include the beam, the 'Brazilian' disc and the disc subjected to axis-symmetrical bending; a shear strength specimen has also been described. The 'fracture envelope' concept has been introduced and a summary of a statistical approach to the processing of test data has been given. Test techniques for other relevant mechanical properties have been outlined and reference has been made to alternative stress analysis techniques for arbitrarily shaped compacts.

## References

- Astley, R.J., 1992. Finite Elements in Solids and Structures: An Introduction. Chapman and Hall, London.
- Awaji, H., Sato, S., 1979. Diametral compression testing method. *J. Engng. Mat. Technol. (ASME)* 101, 139–147.
- Benham, P.P., Crawford, R.J., Armstrong, C.G., 1996. Mechanics of Engineering Materials. Longman Group, Harlow, UK.
- Carneiro, F.F.L., Barcellos, A., 1953. Tensile strength of concrete. *RILEM Bull.* 18, 99–107.
- Case, J., Chilver, Lord, A.H., Ross, C.T.F., 1993. Strength of Materials and Structures. Edward Arnold, London.
- Church, M.S., 1984. Mechanical Characterisation of Pharmaceutical Powder Compacts. Ph.D. Thesis, University of Nottingham, UK.
- David, S.T., Augsburger, L.L., 1974. Flexure test for determination of tablet tensile strength. *J. Pharm. Sci.* 62, 933–936.
- Den Hartog, J.P., 1952. Advanced Strength of Materials. McGraw-Hill, New York.
- Dukes, W.H., 1971. Handbook of Brittle Material Design Technology. AGARDograph No. 152, (AGARD-AG-152-71), North Atlantic Treaty Organisation, (February).
- Durelli, A.J., Riley, W.F., 1965. Introduction to Photomechanics. Prentice-Hall, New Jersey.
- Dwight, H.B., 1961. Tables of Integrals and Other Mathematical Data. Macmillan, New York.
- Fell, J.T., Newton, J.M., 1970. Determination of tablet strength by diametral compression test. *J. Pharm. Sci.* 59, 688–691.
- Hondros, G., 1959. The evaluation of Poisson's ratio and modulus of materials of a low tensile resistance by the Brazilian (indirect tensile) test with particular reference to concrete. *Aust. J. Appl. Sci.* 10, 243–268.
- Kennerley, J.W., Newton, J.M., Stanley, P., 1982. A modified Weibull treatment for the analysis of strength-test data from non-identical brittle specimens. *J. Mater. Sci.* 17, 2947–2954.
- Pitt, K.G., Newton, J.M., Stanley, P., 1988. Tensile fracture of doubly-convex cylindrical discs under diametral loading. *J. Mater. Sci.* 23, 2723–2728.
- Pitt, K.G., Newton, J.M., Stanley, P., 1989a. Stress distributions in doubly convex cylindrical discs under diametral loading. *J. Phys. D: Appl. Phys.* 22, 1114–1127.
- Pitt, K.G., Newton, J.M., Richardson, R., Stanley, P., 1989b. The material tensile strength of convex-faced aspirin tablets. *J. Pharm. Pharmacol.* 41, 289–292.
- Priddle, E.K., 1969. Effect of multiaxial stresses on the fracture strength of silicon carbide. *J. Strain Anal.* 4, 81–87.
- Rabie, A.M., 1981. The Development of a Model Technique for the Design of Brittle Components. Ph.D. Thesis, University of Nottingham, UK.
- Stanley, P., 1977. Methods and practice for stress and strain measurement, Part 2. British Society for Strain Measurement Monograph, pp. 35–43.
- Stanley, P., 1991. The graphical interpretation of fracture load data for doubly-convex cylindrical discs. *J. Mater. Sci.* 26, 2195–2198.
- Stanley, P., 1992. The ball-loaded, ball-supported disc as a strength test specimen for brittle materials. *Materialprüfung* 34, 173–176.
- Stanley, P., Newton, J.M., 1977. Variability in the strength of powder compacts. *J. Powder Bulk Sol. Technol.* 1, 13–19.
- Stanley, P., Sivill, A.D., 1978. On the biaxial fracture of reaction-bonded silicon nitride. *Proc. Br. Ceram. Soc.* 26, 99–111.
- Stanley, P., Newton, J.M., 1980. The tensile fracture stress of capsule-shaped tablets. *J. Pharm. Pharmacol.* 32, 852–854.
- Stanley, P., Inanc, E.Y., 1984. Assessment of surface strength and bulk strength of a typical brittle material. In: IUTAM Symposium on Probabilistic Methods in the Mechanics of Solids and Structures, Stockholm, Sweden, pp. 231–240.
- Stanley, P., Karroum, C., 1992. An evaluation of mechanical strength test specimens for brittle materials. *J. Strain Anal.* 27, 101–111.
- Stanley, P., Sivill, A.D., Fessler, H., 1976. The unit strength concept in the interpretation of beam test results for brittle materials. *Proc. I. Mech. E* 190 (49/76), 585–595.
- Weibull, W., 1951. A statistical distribution function of wide applicability. *J. Appl. Mech.* 18, 293–297.